Plant, Cell and Environment (2004) **27**, 551–567

Whole tree xylem sap flow responses to multiple environmental variables in a wet tropical forest

J. J. O'BRIEN[1], S. F. OBERBAUER[1,2] & D. B. CLARK[3]

[1]Department of Biological Sciences, Florida International University, Miami, FL, 33199, USA, [2]Fairchild Tropical Garden, 11935 Old Cutler Road, Miami, FL 33156, USA and [3]Department of Biology, University of Missouri-St. Louis, St. Louis, MO 63121, USA

ABSTRACT

In order to quantify and characterize the variance in rainforest tree physiology, whole tree sap flow responses to local environmental conditions were investigated in 10 species of trees with diverse traits at La Selva Biological Station, Costa Rica. A simple model was developed to predict tree sap flow responses to a synthetic environmental variable generated by a principle components analysis. The best fit was obtained with a sigmoid function which explained between 74 and 93% of the variation in sap flux of individual trees. Sap flow reached an asymptote where higher light and evaporative demand did not cause sap flux to increase further. Soil moisture had little influence on sap flux. The morphological characteristics of the trees significantly affected sap flow; taller trees responded to changes in environmental variables sooner than shorter trees and high liana cover buffered tree sap flow responses to weather. The effect of species-specific differences on the model was small; the mean effectiveness of the model was reduced by 6% when parameters were estimated from a single pool of measurements taken from all individuals. The results indicate that sap flow response could be effectively estimated using a simple general model and composite environmental index for these 10 diverse tree species.

Key-words: Costa Rica; La Selva; principal components analysis; soil moisture; thermal dissipation probe; transpiration; tropical rainforest; vapour pressure deficit; whole tree water use.

INTRODUCTION

Tropical rainforests are renowned for their high tree species diversity. The diversity of these trees is reflected in their varying life histories, architecture, morphology and physiology, which in turn combine to create a complex forest structure. How these complex characteristics interact to impact whole-tree physiological function is just beginning to be understood. The regulation of transpiration in rainforest trees might be expected to vary strongly among species due to both differences in physiological responses and morphology such as crown architecture, leaf size and shape, among other characteristics. However, Meinzer, Goldstein & Andrade (2001) and Andrade *et al*. (1998) have shown that in some species, variation in transpiration was governed largely by tree size and hydraulic architecture rather than species-specific physiological differences when measurements were scaled to the level of an entire tree. Nevertheless, the potential variation in physiological responses in trees of the same size could be large. Knowledge of the magnitude of any differences among species responses is necessary before individual tree measurements can be scaled up to the stand level. Accurate estimates of stand-level transpiration therefore depend on understanding the source of the majority of variation in transpiration estimates.

Climatic variables that may influence sap flow include radiation, vapour pressure deficit (VPD), soil moisture, rainfall, temperature, wind speed, and leaf wetness. Fetcher, Oberbauer & Chazden (1994) found VPD greater than 1 kPa reduced stomatal conductance in *Pentaclethra macroloba* in Costa Rican rainforests. Meinzer *et al*. (1993, 1995) and Granier, Huc & Colin (1992) showed that sap flow of several tree species decreased under conditions of high VPD. Periodic soil moisture limitation might be an important force driving yearly variation of productivity in tropical rainforests and has been shown to limit transpiration in other forests (Granier 1987). Smith & McClean (1989) showed that wet leaves drastically reduced photosynthesis. Frequent heavy rainfall is a characteristic of wet tropical forests and water films on leaves inhibit diffusion of gases in and out of stomata. Wind disrupts the canopy boundary layer, increasing coupling to the bulk atmosphere and boundary layer conductance and dries wet leaves (Jarvis & McNaughton 1986; Meinzer & Andrade 1997). These multiple environmental factors have complex interactions with each other and with leaves, crowns and forest canopies. In addition, many of the meteorological variables that affect transpiration rates are typically highly correlated with one another. Some can also interact to have opposite effects on tree physiology. For example, VPD and irradi-

Correspondence: Joseph J. O'Brien, (current address) USDA Forest Service, SRS-4104, 320 Green Street, Athens GA, 30602, USA. E-mail: jjobrien@fs.fed.us

© 2004 Blackwell Publishing Ltd

ance often co-vary but have opposite effects on stomatal aperture. Many physical principles and mechanisms driving transpiration at the leaf and crown level are well understood, especially those focusing on the influences of VPD, and irradiance, and more recently hydraulic architecture (Williams *et al*. 2001). The interaction among these factors with other variables such as leaf wetness, soil moisture and soil temperature and a complicated crown environment are less well understood and are less easy to model physically. Because the integrated impact of multiple variables is what actually drives sap flux responses at the whole tree level, exploiting the underlying structure of co-varying weather data to predict whole tree sap flux responses could be an effective approach especially for comparing species-specific responses. Principal Components Analysis (PCA), is often used to detect and interpret underlying structure in multiple co-varying variables. Furthermore, PCA reduces the dimensionality of a dataset; a correlated set of data are condensed into a few composite variables that retain most of the information found in the original variables. These factors are independent, eliminating covariance among the environmental variables. Just as whole-tree sap flow measurements integrate the many internal factors regulating a tree's transpiration rate, the PCA-derived factors are a synthetic representation of the external environmental variables driving transpiration.

Our goals in this study were to develop and test a simple model to predict whole tree water use using a synthetic environmental variable, to contrast the sap flow responses to environmental variables of several tropical tree species, and to explore how different morphological and ecological traits might affect whole-tree water use. We examined the variance in the model coefficients to estimate the magnitude of species-specific sap flow responses and tested the efficacy of a single general model versus several species-specific models.

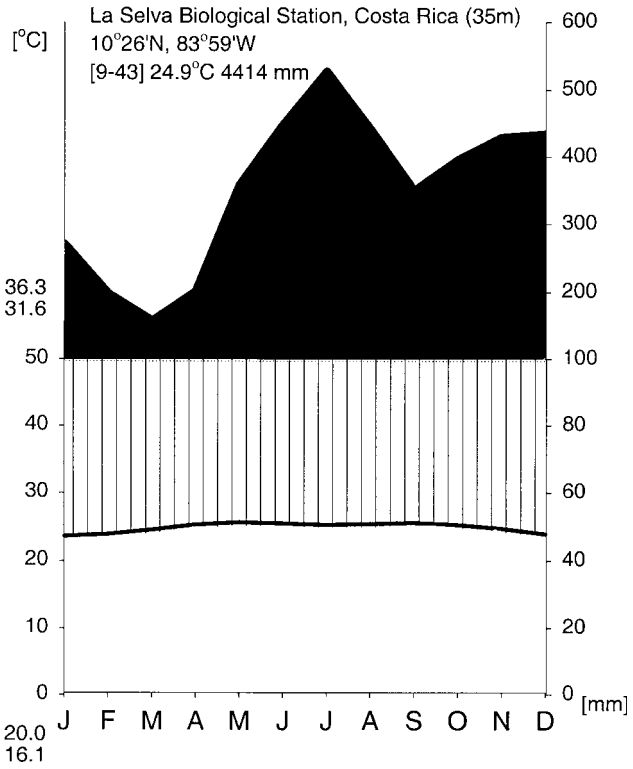

Figure 1. The climate diagram of La Selva after Walter (1985). The diagram highlights the minor annual temperature variation and extremely wet climate of La Selva. Walter (1985) suggested that overlaid plots of rainfall and temperature with *y*-axes where 2 mm of rain equals 1 °C, gave an indication of potential plant water status through time at a site. The resulting plot should be shaded according to the following rules: when the rainfall line dips below the temperature line, stippled fill between the rainfall and temperature lines indicates a water deficit (not shown), the vertical bars indicate humid conditions in which moisture stress is limited, and black fill indicates perhumid conditions, where there is a surplus of water. Throughout the year, monthly averages indicate perhumid conditions prevail at La Selva.

METHODS

Study site and species

We conducted the study at the La Selva Biological Station in north-eastern Costa Rica. The site is in an old-growth, low-elevation (approximately 35 m), tropical, wet, evergreen forest. La Selva receives an average of 4414 mm of rain annually, without a marked dry season (Fig. 1). Similarly, monthly temperature variation is minimal.

We focused on 10 species with diverse life histories ranging from pioneers to giant emergent trees. These 10 species are representatives of four functional groups and show a wide range of morphological and life history traits (Clark & Clark 1992). The leaf morphology, wood anatomy and growth rates vary among the species, as do leaf and reproductive phenology and tree longevity (Frankie, Baker & Opler 1974; Clark & Clark 1999). A summary of the range in traits likely to influence whole tree water use are found in Table 1. These 10 species constitute a large proportion of the forest biomass; one of the species, *Pentaclethra macroloba* represents 40% of the timber volume at La Selva (King 1996). With the exception of *P. macroloba*, which they did not include in their study, all of our study trees were a subset of individuals sampled yearly by Clark & Clark (1994). We randomly selected four or more individuals of each species with the criteria that the trees had a well-illuminated crown and a stem diameter above buttresses between 30 and 60 cm Clark & Clark (1999) showed that the fastest growing individuals occur in this size class, with the exception of *Cecropia obtusifolia* (which grows fastest at a slightly smaller diameter). Measuring sap flow in rapidly growing individuals enabled us to better detect tree responses to weather conditions.

Environmental variables

We measured the following micrometeorological parameters on top of a 30 m antenna mast located in the old-growth forest: solar irradiance (silicon pyranometer;

Table 1. The tree taxa and sample size of individuals studied

Family	Species	Leaves	Functional group	Trees sampled	Days measured
Cecropiaceae	*Cecropia insignis* Liebm.	S	D	4	36
	Cecropia obtusifolia Bertol.	S	D	4	42
Euphorbiaceae	*Hyeronima alchorneoides* Allemão	S	C	4	74
Fabaceae	*Balizia elegans* (Ducke) Barneby & J. W. Grimes	c	C	4	68
	Dipteryx panamensis (Pittier) Record & Mell	C	B	4	58
	Hymenolobium mesoamericanum H. C. Lima	c	B	4	95
	Pentaclethra macroloba (Willd.) Kuntze	c		8	136
Lecythidaceae	*Lecythis ampla* Miers	S	A	4	77
Olacaceae	*Minquartia guianensis* Aubl.	S	A	4	78
Simaroubaceae	*Simarouba amara* Aubl.	C	B	4	87

Letters in the leaves column refer to simple (S) and compound (C), capital letters indicate leaves or leaflets longer than 5 cm, lower case indicates leaves or leaflets <5 cm long. The letters in the functional group column refer to the life history categories of Clark & Clark (1992).

Li-200X, Li-Cor Inc, Lincoln, NB, USA), rainfall (TE 525; Texas Electronics, Dallas, TX, USA), wind speed and direction (RM Young Wind Sentry, Traverse City, MI, USA), leaf wetness (247 wetness sensing grid; Campbell Scientific Inc., Logan UT, USA), air temperature and relative humidity (CS500 probe; Campbell Scientific Inc.). We also measured volumetric soil moisture in the top 30 cm of soil (CS615 probe; Campbell Scientific Inc.) and soil temperature at 15 cm using a type-T thermocouple at the tower base. Atmospheric pressure (CS105 barometric pressure sensor; Campbell Scientific Inc.) was measured at a duplicate weather station on top of a 42-m tower located approximately 1 km away. Missing data from the antenna mast were replaced with readings taken from the 42-m tower. At both stations, a Campbell CR10 datalogger read the sensors every 30 s and stored 30-min averages. We calculated VPD using the 30-min averages of temperature and relative humidity after Campbell & Norman (1998). We synchronized all the datalogger clocks to Central Standard Time.

Sap flow measurements

We measured sap velocity by installing a single thermal dissipation probe (TDP) consisting of a pair of 30-mm-long needles into the tree trunks (Granier 1987). We used both commercially manufactured probes (TDP 30; Dynamax Inc., Houston, TX, USA) and self-made probes of similar design. Because the trees we used were part of a long-term demographic study, we installed only one probe to minimize tree injury. We inserted the probe needles into two holes 5 cm apart, drilled into the trunk 1.5–3 m above the ground and any buttresses. We insulated the probes with a 15-cm-diameter polystyrene hemisphere and sealed the probes and the hemisphere to the tree trunk with plastic modelling clay and duct tape. Although the clay around the probes might have caused some error due to heat conductance, the heavy rainfall at the site necessitated sealing the probes to minimize potentially large errors caused by water flowing down the stems and over the probes. An aluminized sheet of plastic bubble-wrap covered the probe and the tree trunk to a point 1.5 m below the probe. The plastic sheet reduced probe error introduced by sunlight heating the trunk (Gutierrez *et al*. 1994). A 36 amp-hour 6 V deep cycle battery coupled to a DC voltage regulator (AVRD regulator; Dynamax Inc.) set at the manufacturer recommended 3 V, provided 0.2 W of power to heat the sensor and caused a maximum temperature difference of approximately 5–8 °C between the heated and unheated needles. The probes were left in place for 2–8 week from 1998 to 2000 and rotated among study trees. Dataloggers (Campbell 21X, CR10, and CR10X) measured the sensors every 30 s and stored 30-min averages of the probe temperature difference. We calculated sap flow using the function reported by Granier *et al*. (1992) and recommended by the probe manufacturer. This function integrates sap flow over the probe length and calculates sap flux density (J_s) as kg H_2O dm^{-2} h^{-1}.

TDP estimates of xylem sap velocity can show a large degree of variation depending on probe placement (Jiménez *et al*. 2000) and error can be introduced from probe insertion into non-conducting xylem (Clearwater *et al*. 1999). These errors would be superimposed on real differences in the magnitude of J_s among the species. Because of the potential magnitude of these errors was unknown, we chose to focus on analyzing a standardized sap flux density (*SSF*) and focusing on the behaviour of the J_s as measured by a single TDP. We standardized the J_s data for each tree by subtracting the mean for the entire measurement period from each 30-min observation and then dividing the result by the standard deviation (a z score). This procedure resulted in all J_s measurements having a mean of 0 and a standard deviation of 1. In cases where negative values might preclude an analysis such as the function requiring the calculation of a natural logarithm, a positive integer was added to all observations, raising the mean to that integer value and reported the value as $SSF + X$, where X represents the value of the integer.

Sap flow models

In order to construct the PCA-based model we followed this general procedure: First, we extracted PCA factor

scores from all the environmental data, reducing the number of variables to model from nine to three. Second, we generated and saved factor scores from the PCA analysis and matched these data to simultaneous sap flux observations. Finally, we applied a four-parameter sigmoid function with a linear correction to predict sap flux based on the factor scores.

We used the PCA module in Statistica (1999 Edition; StatSoft Inc., Tulsa, OK, USA), to analyse the 30-min micrometeorological data we collected between February 1998 and August 2000 and described above. We applied a varimax rotation to the PCA axes and saved the factor scores. Rotating the axes maximizes the differences in loadings among axes and makes interpretation of the underlying structure easier. The factor scores are the sum of the product of the standardized environmental variables and their respective rotated axis factor loadings. Each 30-min observation of the environmental data had an associated factor score and could be matched to sap flux observations taken at the same time. We chose to use a four-parameter sigmoid function to model the sap flux data (described in detail below). Empirically, we saw that plots of sap flux versus the factor scores showed an obvious S-shaped pattern. We chose a four-parameter function for theoretical reasons since each parameter represented an important physiological response. These were the function extrema, at which environmental factors had little effect on sap flux, the conditions where there was a linear change of sap flux in response to climatic drivers, and the influence of rainfall on leaves as a physical barrier to water vapour movement out of stomata. Furthermore, we could use the extrema of the second derivative of the function, where sap flux was initiated and where environmental drivers began to lose effect as points to compare among species.

Sap flux lags and hysteresis

Because lags between transpiration from the crown and sap flow at the base of tree could complicate modelling of sap flux in relation to canopy microclimate, we examined plots of hysteresis between sap flux and important environmental variables to confirm the presence of lags. We also tested for differences between the timing of maximum sap flow and the environmental variables. Although lags may have been present, we assumed that any lags would be similar among species because the study trees were of similar size and height (Goldstein *et al*. 1998). We also analysed integrated J_s over a 24-h period to compare the impact of lags in modelling the J_s response to environmental variables.

Transpiration estimates

To estimate whole-tree transpiration from TDP measurements, estimates of the active sapwood area are required. Sapwood area is usually determined using a stem core sample extracted at the point of TDP insertion. In order to minimize tree damage, we chose not to determine sapwood depth directly. For two species, *Minquartia guianensis* and *Simarouba amara*, we calculated tree transpiration using sapwood area estimates from published diameter–sapwood relationships (Ryan *et al*. 1994). For these species we also estimated crown conductance (g_c) after Meinzer & Andrade (1997). As we did not measure leaf temperature, we assumed leaf and air temperature were equivalent in our calculations of vapour pressure difference between leaf and air.

Statistical analyses

We suspected that differences among species responses might be partly explained by tree canopy idiosyncrasies, therefore we analysed the model coefficients with a multivariate analysis of covariance (MANCOVA) with SPSS (Release 10.0.5; SPSS Inc., Chicago, IL, USA), using liana cover, a crown area index and crown height above neighbouring tree canopies as covariates. We measured liana cover by visually assessing the proportion of the crown occupied by lianas in six classes (0, 0–5, 5–25, 25–50, 50–75 and >75%). We estimated crown area by measuring distance from the edge of the canopy to the trunk in four cardinal directions and then calculated the crown area as if it were an ellipse. We assigned each tree a canopy height index based on a z score calculated from fast laser imaging-mobile airborne platform (FLI-MAP) data collected in September 1997 (US National Aeronautics and Space Administration, unpublished results). The FLI-MAP canopy heights were extrapolated from a digital terrain model generated by laser vegetation imaging sensor (LVIS) data also collected in 1997 (Weishampel *et al*. 2000; Drake *et al*. 2002). Each pixel in the FLI-MAP model represents the elevation of a 0.3 m^2 area. To create the height index, we estimated the crown elevation for each individual tree by averaging the pixel values found in a 5-m-radius circle centred on its bole, which would encompass the majority of the crown area. We then calculated the average and standard deviation of pixel values in a 75-m-radius circle centred on the tree bole. The canopy height index, calculated as a z score, indicated whether the tree was embedded in or emergent from the surrounding canopy and therefore estimated potential canopy coupling with the atmosphere. Tall trees had high index values, and trees embedded in the forest canopy had low index values. Two trees were not covered by the FLI-MAP survey; therefore we substituted the species means for these missing values.

RESULTS

Species characteristics

Mean values of the species bole diameter, crown area, crown height index, and liana cover differed significantly among species, although with large overlaps (Table 2, Fig. 2). For bole diameter, two groups of two species differed from each other: *C. obtusifolia* and *Hyeronima alchorneoides* were significantly smaller than *Dipteryx panamensis* and *Lecythis ampla* individuals, although neither

Table 2. ANOVA results of comparison of species mean bole and crown characteristics

Dependent variable	Type III sum of squares	Mean square	*F*	*P*-value
Crown projection	90670.66	10074.52	3.23	0.01
Crown height index	13.16	1.46	3.86	0.00
% Liana cover	16298.35	1810.93	4.15	0.00
Bole diameter	1680.28	186.70	2.45	0.03

species within the group differed from each other or any of the other species. *Cecropia obtusifolia* had a significantly smaller crown than either *D. panamensis* or *L. ampla* individuals, although there were no differences among all other combinations of species. The crown height index differed among four species: *Cecropia insignis* and *H. alchorneoides* crowns were lower in the canopy than *D. panamensis* trees, and *C. insignis* crowns were lower than *S. amara* crowns. Liana cover did not differ among nine of the 10 species; only *M. guianensis* had significantly more liana cover than five other species.

Environmental variables

Nearly all the weather variables were correlated to some degree (Table 3, Fig. 3). Soil temperature and soil moisture were only moderately correlated with air temperature and soil temperature. Rainfall was not correlated with any variable at the 30-min time scale. The factor loadings in the PCA mirrored these patterns of correlation. The first three PCA axes explained 77% of the variance in the complete data set (Table 4). The first axis explained 48% of the variance in the data and was positively correlated with irradiance, VPD, air temperature and wind speed and negatively correlated to relative humidity and leaf wetness. High values of axis 1 scores occurred on sunny, dry, warm, windy days, creating conditions of high evaporative demand, so we referred to this factor as the evaporative demand index (EDI, Table 5). The second axis explained an additional 18% of variance and was positively correlated with the soil moisture and soil temperature, so we referred to it as the soil index. The third axis explained a further 12% of the variance and was correlated only to rainfall, so we called it the rain index.

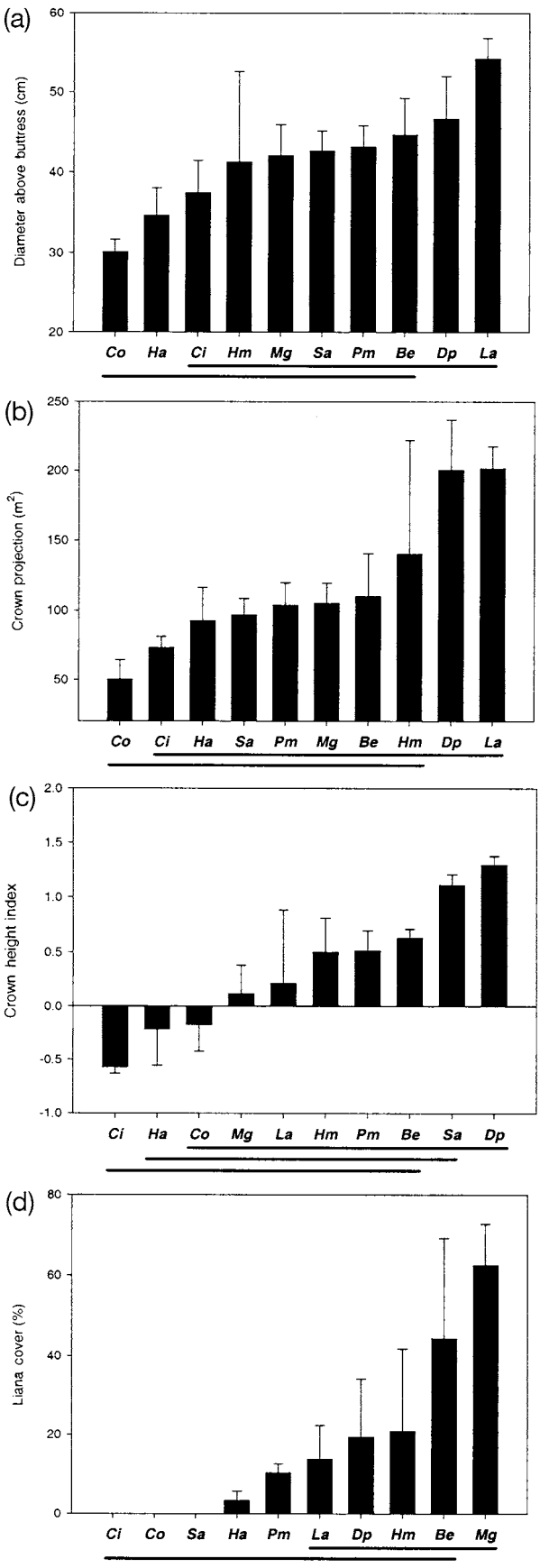

Figure 2. Plots of mean bole diameter above buttress (a), crown projection (b), crown height index (c), and liana cover (d) for all 10 species. Crown projection was calculated by assuming an elliptical crown and measuring the major and minor axes. The crown height index represented the position of the tree crown relative to crown heights of neighbouring trees calculated from remotely sensed data. Positive values indicated emergent trees, values close to 0 or negative indicated crowns at or below mean canopy level. Liana cover was estimated as a percentage of the total crown occupied by liana leaves. The whiskers represent 1 standard error of the mean. A solid line below the species abbreviations indicates the means did not differ (Tukey's HSD, $P > 0.05$).

Table 3. Correlations among the 30-min averages of weather variables measured during the study period are shown below. Coefficients less than 0.2 are marked with an *x*

N = 40 500	Irradiance	Air Temp.	Relative humidity	VPD	Leaf wetness	Wind speed	Rain	Soil moisture
Soil temperature	*x*	0.51	*x*	*x*	*x*	*x*	*x*	–0.42
Irradiance		0.73	–0.76	0.76	–0.37	0.63	*x*	*x*
Air temperature			–0.85	0.87	–0.48	0.56	*x*	–0.24
RH				–0.99	0.53	–0.65	*x*	*x*
VPD					–0.52	0.64	*x*	–0.20
Leaf wetness						–0.34	*x*	–0.29
Wind speed							*x*	*x*
Wind direction							*x*	*x*
Rain								*x*

Sap flux density

The estimates of J_s varied considerably among individuals within species. Maximum sap flux ranged from 2.43 to 6.86 kg H_2O dm^{-2} h^{-1} (Table 6). In all species, the highest sap flow occurred around noon, although timing of peak flow varied depending on weather conditions such as rainfall. The pattern of variation in sap flow closely matched the pattern of variation in the EDI, but there was little congruence among the patterns of sap flow and the soil and rain factors.

Sap flux lags and hysteresis

The time of maximum J_s was either coincident or occurred after maximum irradiance (Table 7). Maximum J_s occurred

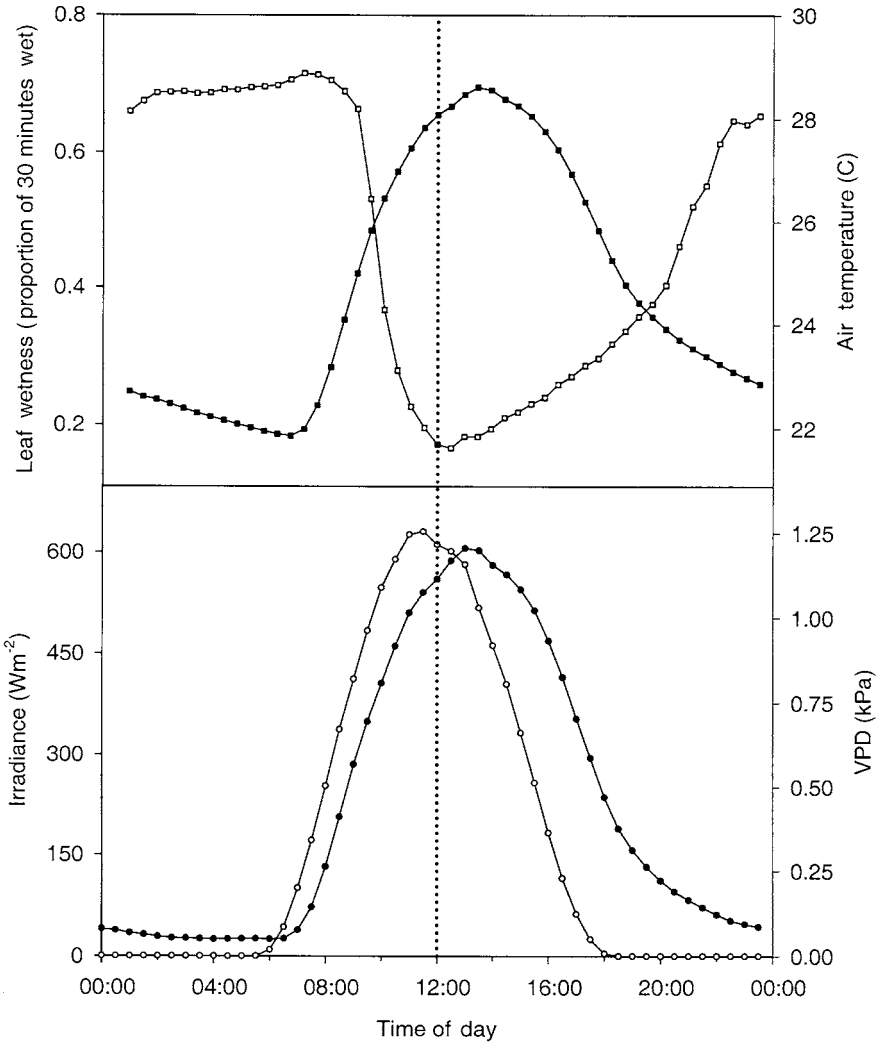

Figure 3. Mean 30-min weather observations for air temperature, leaf wetness, VPD and irradiance over the study period (1997–2000). The high degree of correlation is evident among irradiance (○), air temperature (■), and VPD (●). Leaf wetness (□) was inversely correlated with each of the previously mentioned variables. Leaves are wetted by heavy dewfall, which occurred nearly nightly, and began drying approximately 2 h following sunrise. The vertical dotted line represents noon.

Table 4. Eigenvalues and the variance explained by the first three axes of the PCA on the weather data

Axis number	Eigenvalue	% Total variance explained	Cumulative eigenvalue	Cumulative % variance explained
1	4.32	48	4.32	48
2	1.57	18	5.9	66
3	1.03	12	6.93	77

earlier than maximum VPD in all species. The timing of maximum EDI was either coincident or after maximum J_s. Plots of 30-min mean J_s versus irradiance, VPD, and EDI revealed a counter-clockwise hysteresis for irradiance, but a clockwise hysteresis for VPD and EDI (Fig. 4). These patterns were consistent for all species. Hysteresis was eliminated or significantly reduced in the EDI plots. In order to separate the effects of light and evaporative demand we plotted the normalized J_s response to VPD in a manner similar to Meinzer *et al*. (1995). Meinzer *et al*. divided VPD values by simultaneous irradiance measurements to control for the effect of light on the behaviour of stomata. When plotting 30-min values, all species showed a unimodal response with a positive skew indicating an initial increase in sap flow with higher VPD, followed by a rapid decline (Fig. 5).

Table 5. Factor loadings of the environmental variables on the first three PCA axes

Variable	Factor 1 'EDI'	Factor 2 'Soil'	Factor 3 'Rain
Soil temperature	0.13	–0.81	0.08
Irradiance	0.84	0.05	0.00
Air temperature	0.90	–0.34	–0.02
Relative humidity	–0.96	0.05	0.09
VPD	0.96	–0.09	–0.08
Leaf wetness	–0.62	–0.37	0.14
Wind speed	0.72	0.08	0.20
Rainfall	–0.06	0.02	0.98
Soil moisture	–0.10	0.83	0.12

The loadings are analogous to Pearson correlation coefficients. High loadings (greater in magnitude than 0.6 and underlined) were used in the interpretation and naming of the factors, the names in quotes represent our interpretation of the structure.

Crown conductance

Crown conductance was higher in *S. amara* than *M. guianensis* (Fig. 6). The pattern of g_c against VPD was similar to that of the J_s response, and g_c increased as a quadratic function of VPD (Fig. 7). The responses differed slightly between the species, mostly due to the differences in the magnitude of g_c. The response of g_c to irradiance was best explained by a linear function (Fig. 7). The slopes differed between the species with *S. amara* having a steeper response function than *M. guianensis*. The differences between these two species probably reflect both differences in sapwood area (*S. amara* had about twice the sapwood area, Ryan *et al*. 1994), but also in the crown characteristics. The crowns of *S. amara* trees are much more open and less

Table 7. Mean lag (minutes) of environmental values relative to maximum sap flow

Species	Irradiance	VPD	EDI
Pm	73.9*	–28.7*	15.5
Sa	69.4*	–35.4*	18.7
Be	68.7*	–23.3*	10
Ci	4.95	–109.8*	–39.6
Mg	56.5*	–41.3*	–1.8
La	9.3	–75.2*	–38.9*
Ha	37.8*	–78.26*	–28*
Hm	29.2*	–77*	–26*
Dp	–21	–122.3*	–79.5*
Co	16.4	–105*	–65*

The values were calculated as the number of minutes between when the maximum J_s occurred minus when the maximum irradiance, VPD, or EDI occurred. Negative values indicate maximum J_s occurred before the environmental variable. Values with asterisks had mean differences significantly different than 0 ($P < 0.05$).

Table 6. J_s averaged over the entire measurement period (kg H_2O dm^{-2} h^{-1}) for the 10 species

Species	*n* (trees)	*n* (30-min means)	Mean	Standard error	Maximum
B. elegans	4	3564	0.84	0.61	4.22
C. insignis	5	1728	0.54	0.43	5.64
C. obtusifolia	4	2016	0.41	0.40	3.30
D. panamensis	4	2784	0.94	0.67	4.77
H. alchorneoides	4	3552	0.62	0.47	3.46
H. mesoamericanum	4	4560	0.77	0.62	5.93
L. ampla	4	3696	0.82	0.57	4.94
M. guianensis	4	3744	0.29	0.29	2.43
P. macroloba	8	6528	1.00	0.32	6.86
S. amara	4	4176	0.41	0.33	4.45

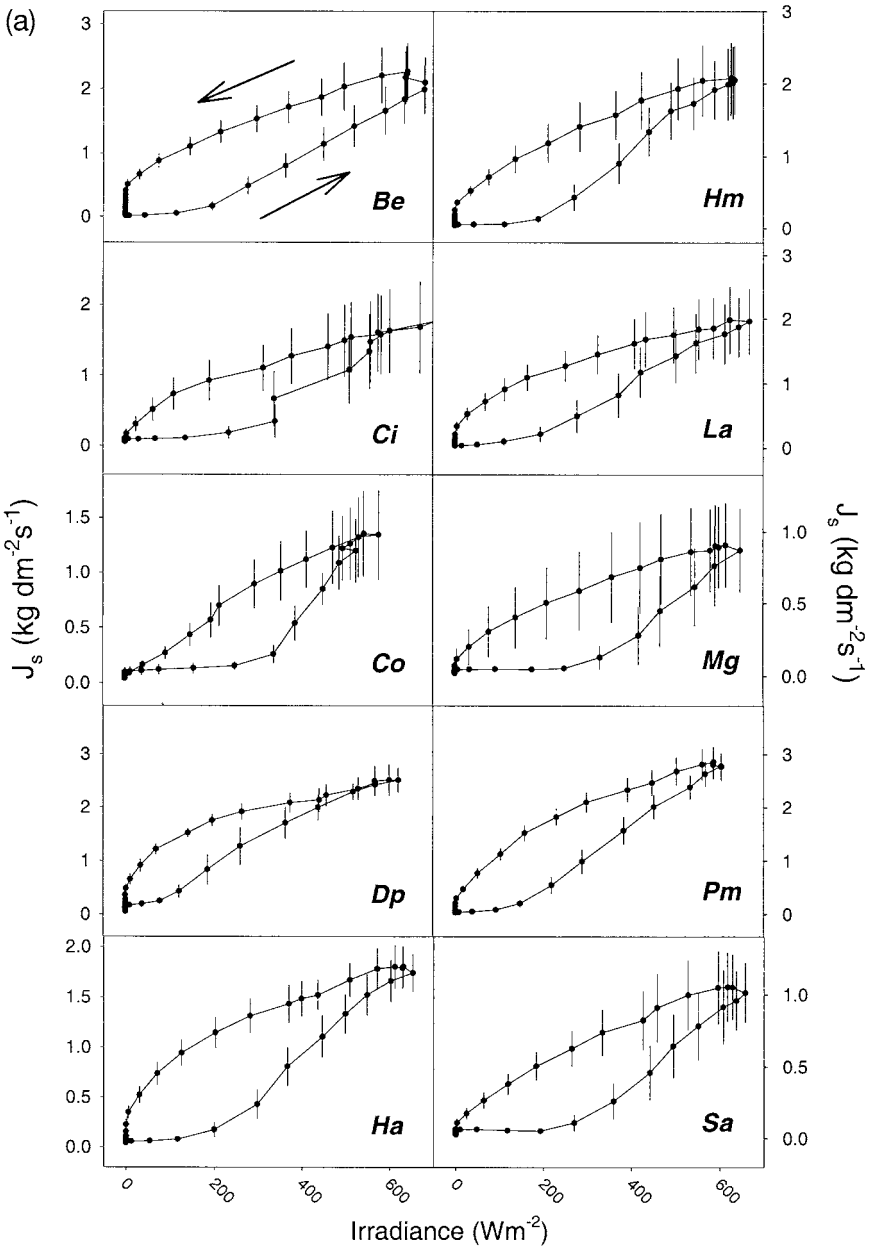

Figure 4. Plots of 30-min mean J_s plotted against irradiance (a), VPD (b) and EDI (c). The points in the plots represent 30-min means, the arrows in the upper left plot (*Be*) represent the direction where the next consecutive observation in time occurred. The direction of sap flux hysteresis in all species was counterclockwise for irradiance, but clockwise for VPD and EDI. The whiskers are 1 standard error.

dense than *M. guianensis* crowns. Furthermore, liana cover was much higher in *M. guianensis* and might affect the crown boundary layer characteristics.

Sap flux models

The four-parameter function explained 74–94% of the variation in *SSF* (Fig. 8). We then examined the residuals of this model, and found a negative linear correlation with the rain index, but no correlation with the soil index. Since the soil index was uncorrelated with the residuals of the non-linear function, we did not include it in any further analyses. We included a rainfall correction coefficient to the sigmoid function and re-estimated the parameters. The final form of the model was:

$$SSF = y_o + \frac{a}{1 + e^{-\left(\frac{x - x_o}{b}\right)}} + cz \quad (1)$$

The independent variables were the EDI (x) and the rain index scores (z). The estimated parameters were the function low value (y_o), the function high value (a), the inflection point (x_o), the slope of the transition (b), and the correction coefficient for rainfall (c).

This function has two asymptotes, where changes in EDI had little influence on sap flux. Sap flux changed little at night or under dark, still, humid conditions, then increased rapidly in a nearly linear fashion as conditions became warmer, brighter, drier and windier. It approached an upper asymptote when maximum sap fluxes were achieved and higher values of these weather conditions had little

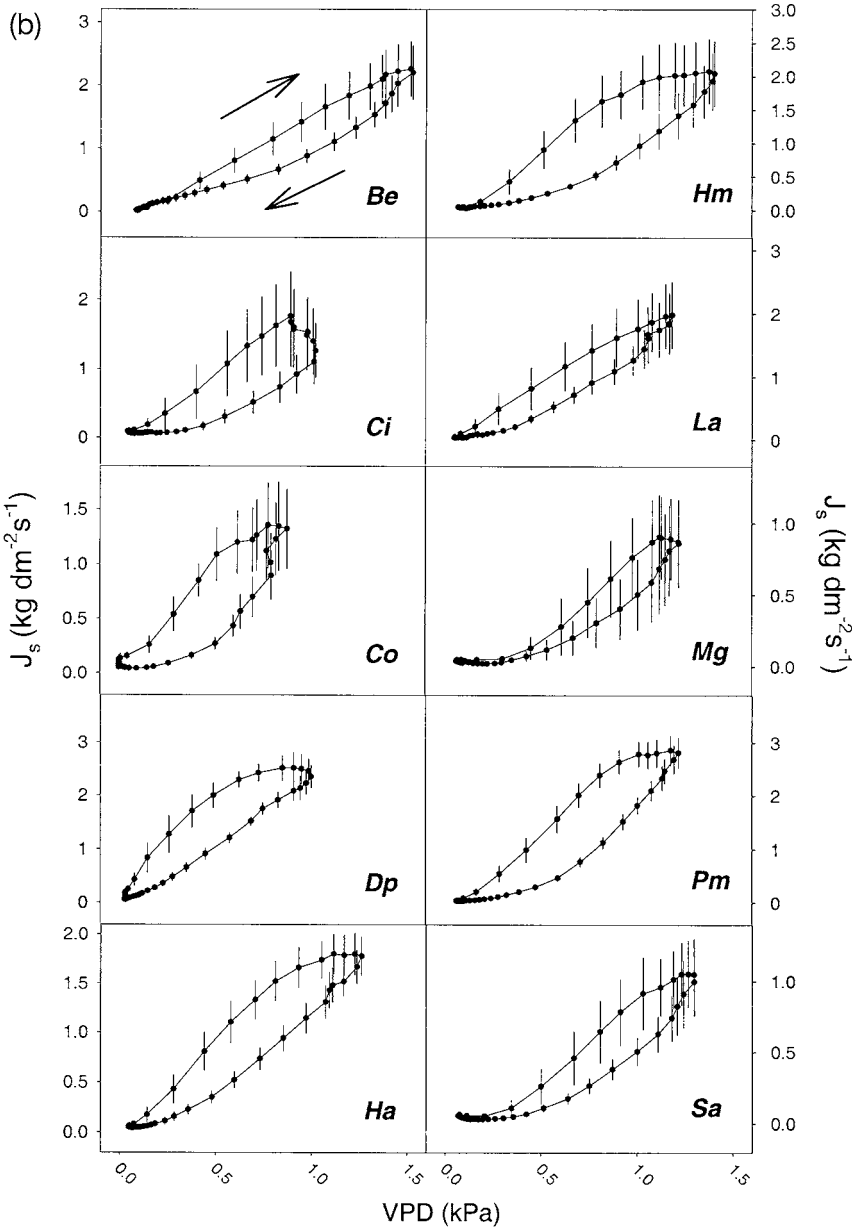

Figure 4. *Cont.*

effect (Fig. 9). Rainfall always reduced sap flow. Since the model showed two asymptotes separated by a nearly linear change in sap flux rates, comparing the maximum and minimum of the second derivative provided an independent point to test for differences among species in initiation and termination of sap flux responses to the climatic conditions. These points occurred where the maximum increase and decrease in transpiration rate occurred (Fig. 9). We also included the EDI values at these extreme points in the analysis of the model parameters among species (Table 8).

We tested the model parameters and crown characteristics for violations of the analysis of covariance assumption of homogeneous slopes by examining the interaction between the species and covariates. None of the tests were significant ($P > 0.5$). The MANCOVA showed that liana cover had a significant positive linear relationship with the model inflection point and the two points where maximum transpiration rate changes occurred (Table 9). Canopy height index exhibited a significant negative relationship with the function maximum values (Table 9). More exposed canopies had lower function maxima, indicating that *SSF* began to increase at lower values of the EDI. Crown area was not significantly correlated to any of the parameters despite the four-fold range in crown area among species.

After adjusting for the effects of liana cover and crown exposure with the MANCOVA, we found significant differences among the species in the means of four of the model parameters (Table 10). In all cases however, the differences were a continuum with no significant outliers (Table 11). Despite the small differences in a few parameters among a few of the species, the responses to the EDI appear similar among all the species (Fig. 10). The *Balizia elegans*

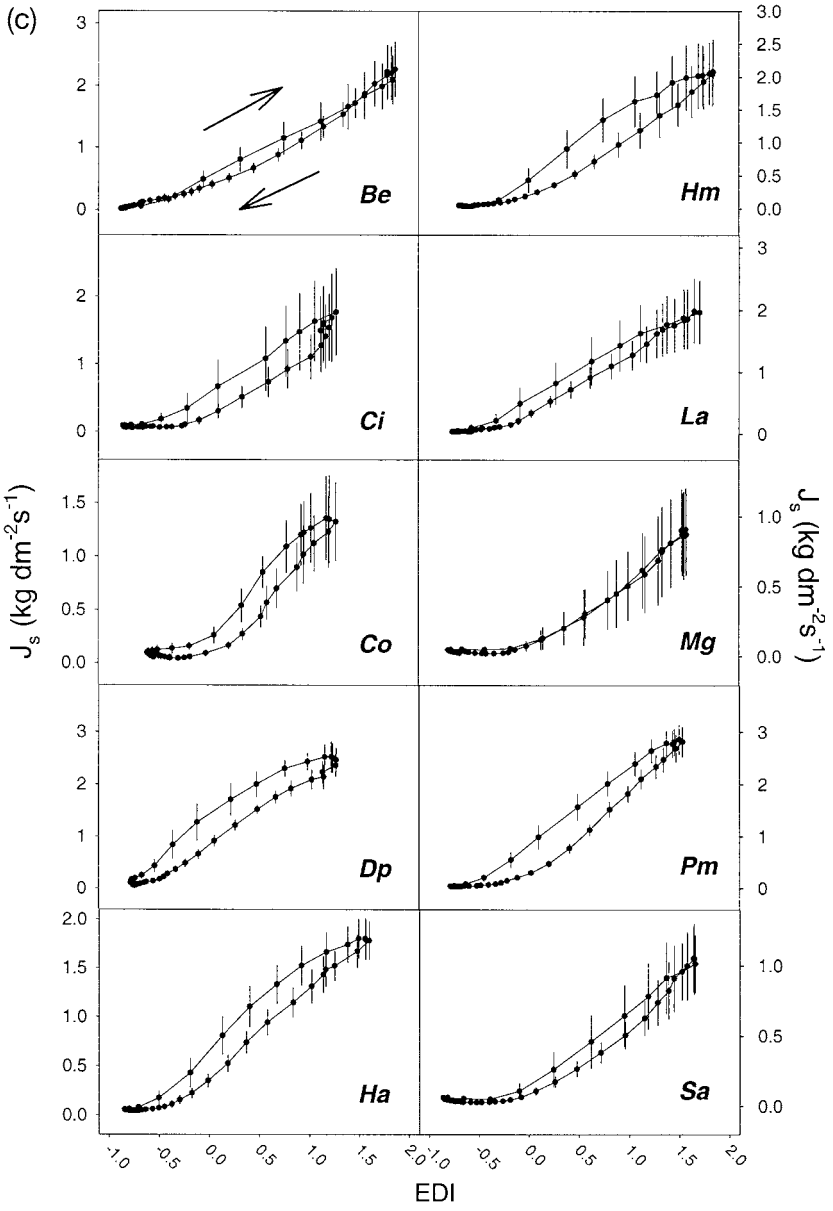

Figure 4. *Cont.*

response curve tended to be flatter than the other species although its slope parameter did not differ from that of *Hymenolobium mesoamericanum* and *L. ampla*, which were not statistically different from the rest of the taxa. The upper asymptote in *B. elegans* was higher than *H. alchorneoides*, although the *post hoc* tests showed that the rest of the species overlapped with both. *Dipteryx panamensis* and *S. amara* showed the same pattern for the value of the lower asymptote; *D. panamensis* had a lower value than *S. amara* but neither differed from the rest. *Dipteryx panamensis* also reached the upper asymptote at lower EDI values than *H. mesoamericanum*, *S. amara* and *B. elegans*, but did not differ from the rest.

To estimate the sensitivity of the sap flow model to the species-specific differences described above, we recalculated parameters, pooling tree measurements at different levels and compared the variance explained. First, we estimated model parameters for each individual and then averaged the R^2 by species. We then generated the estimates from a pool of all individuals within a species and finally pooled all individuals from all species. Individual differences accounted for approximately 3% of the model efficiency and species level differences accounted for an additional 3%. Pooling all individuals reduced the average variance explained by approximately 6% (Table 12).

DISCUSSION

Our results showed that we could effectively model short-term tree sap flux responses with a sigmoid function using synthetic climatic variables as predictors. Our multivariate

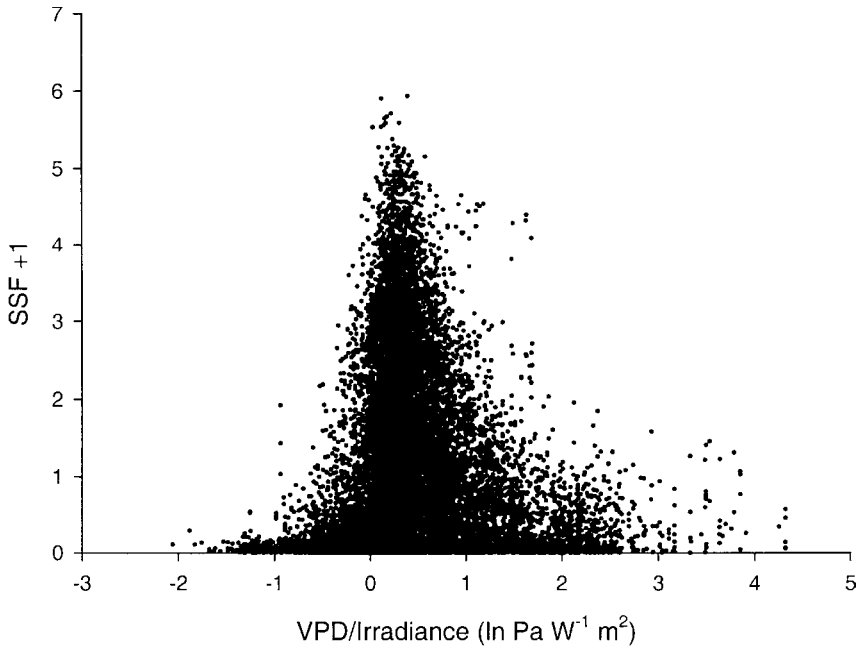

Figure 5. Plots of mean daily J_s against normalized VPD (VPD/irradiance) over the entire study period. The data were plotted after taking the natural logarithm of the normalized VPD values. Each point represents a 30-min mean from a single tree. All species are plotted together.

approach simplified the model and ensured the independence of the explanatory variables. The model performed well, explaining an average of 74 to 93% of the variance in sap flow for the 10 species and explained an average of 89% of the variance across all species. The greatest discrepancies between measured and predicted flux occurred under conditions of low sap flow and at night. Ewers & Oren (2000) found relatively higher TDP error under conditions of low sap flow and low VPD, suggesting that flux measurement error might partly explain the lower model performance under these conditions. Nevertheless, night-time stomatal closure also explains why the model consistently overestimated sap flux during the rare nights with high evaporative demand.

The species we measured had remarkably similar response patterns to the climatic conditions (Fig. 10). Although the model parameter means differed among a few of the taxa, the effect size was small as indicated by the minor decrease in model efficacy when we derived parameter estimates from a pool of all individuals (Table 12). These species with widely varying morphology, anatomy, life history and architecture appear to have converged on a common response to environmental conditions. Meinzer *et al*. (2001) found convergence in the relationship between

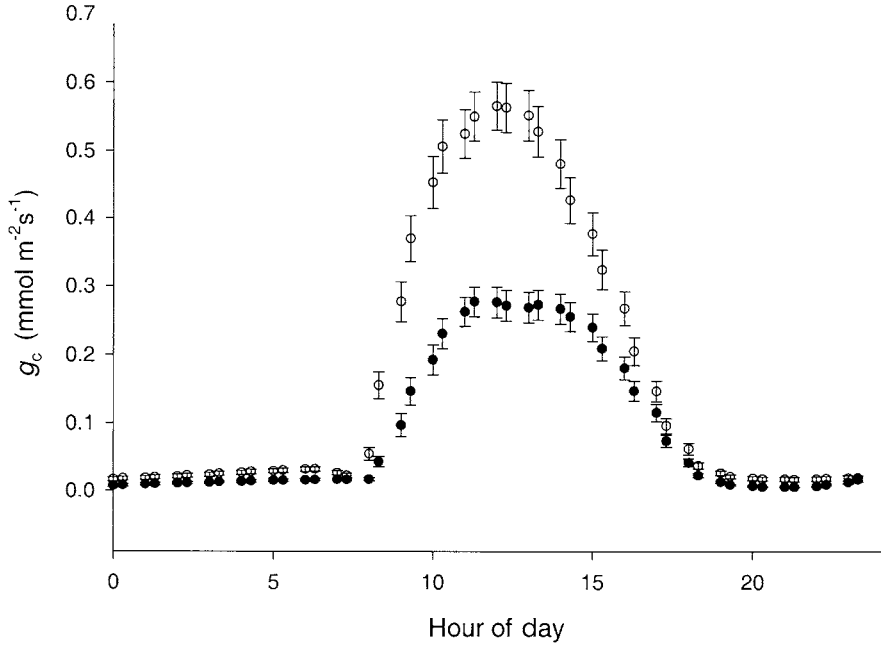

Figure 6. Time course of mean hourly values of g_c for *S. amara* (○) and *M. guianensis* (●). The means represent 87 d of observations for *S. amara* and 78 d for *M. guianensis*. The whiskers represent 1 standard error.

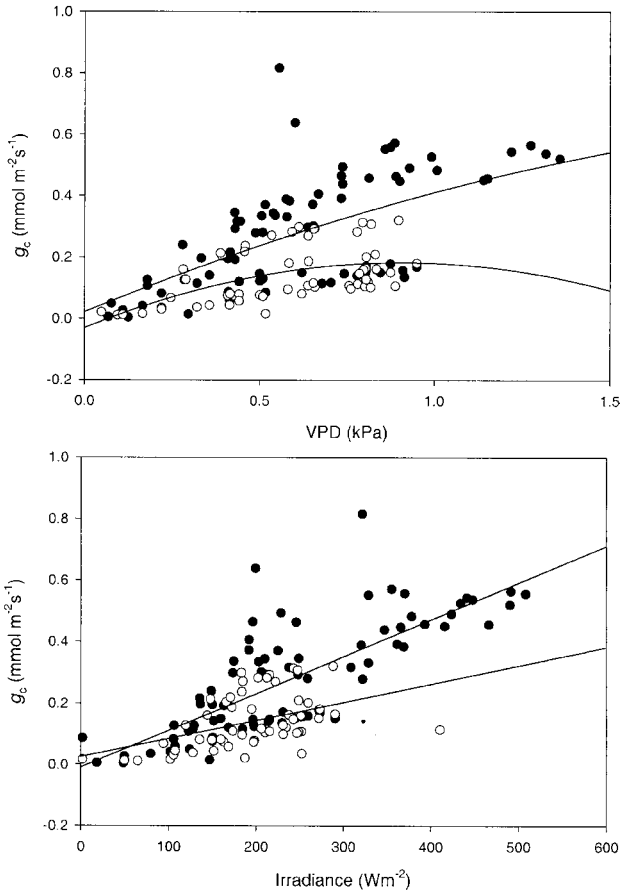

Figure 7. Time course of mean daily g_c of *S. amara* (○, n = 87 d) and *M. guianensis* (●, n = 78 d) plotted against matched mean daily values of irradiance and VPD. The R^2 values for the regression lines for *S. amara* were 0.40 (VPD) and 0.58 (irradiance). The R^2 values for the regression lines for *M. guianensis* were 0.31 (VPD) and 0.45 (irradiance).

water transport and sapwood area in species with widely varying xylem morphology. They suggested that the relationship between sap flow and evaporative demand might show a similar universality among species. Our results support this view.

A further reason for the similarity among species responses may be that under some conditions, physiological responses are not the primary determinants of water loss from the canopy. In tropical moist forest in Panama, stomatal responses of trees in gaps were found to be largely uncoupled (*sensu* Jarvis & McNaughton 1986) from the whole tree transpiration because canopy conductance was often lower than stomatal conductance (Meinzer *et al.* 1995; Meinzer & Andrade 1997). The same uncoupling may have occurred in our study. Consequently, water loss from the canopy may have been strongly influenced by climatic conditions, resulting in similar responses. As we were unable to compare absolute values of sap flow among species due to our sampling limitations, we cannot say whether the volume of whole tree water use in this wet tropical forest was independent of species. We can say that climate affected sap fluxes similarly among these species. This could be an effect of measurement scale, not a lack of intrinsic differences in physiology (Andrade *et al.* 1998; Meinzer *et al.* 2001); nevertheless, the similar responses among species would simplify sampling efforts when estimating stand transpiration.

Elucidation of specific factors driving transpiration of individual trees is typically hampered by covariance and interaction among the environmental drivers. An alternative to our PCA approach is to use physiologically based functions to fit the data and analyse the responses of the residuals. When we fit a light response model, the model explained 70% of the variation in the sap flow data (data not shown), considerably less than the sigmoid EDI model. Analysis of the residuals of the light response model still

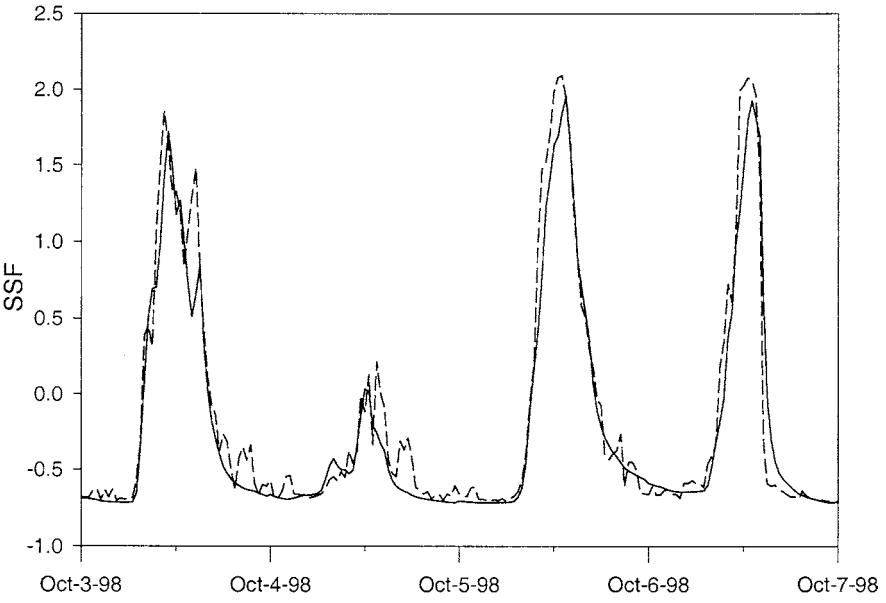

Figure 8. An example of the model fit; the plot shows concurrent observed (solid line) and predicted (dashed line) 30-min mean standardized sap flow in a single *B. elegans* tree over a period of 4 d in October 1998. The predicted sap flux values were generated using the 30-min EDI and the parameters for eqn (1) as reported in Table 8.

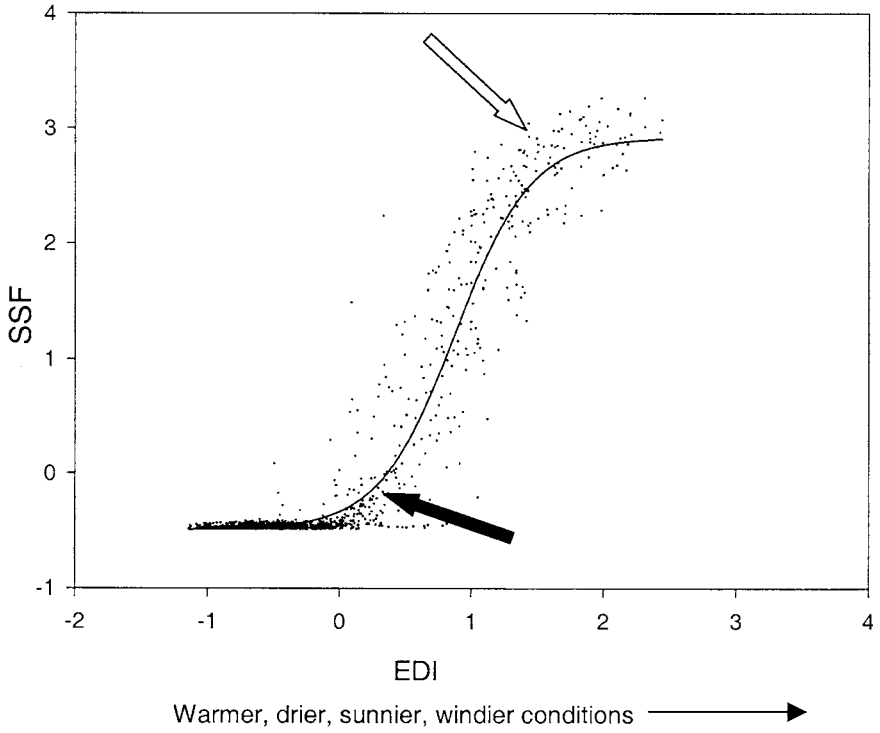

Figure 9. A plot of 44 d of standardized 30-min sap flow observations of a *Pentaclethra macroloba* tree taken in October 1999 and December 1999–January 2000. The solid line represents the predicted standardized sap flow predicted by eqn (1); the points are the observed 30-min means of standardized sap flow. The arrows indicate the approximate location of the maximum (filled arrow) and minimum (unfilled arrow) values of the function second derivative.

suffered from the covariance problem, which also prevented us from separating the importance of individual environmental variables of the EDI on sap flow. However, through our other analyses, we could infer some mechanisms driving the patterns we observed. J_s was positively correlated with higher irradiance, VPD, temperature, and wind speed, but negatively correlated to leaf wetness.

Although irradiance is known to have positive direct and indirect effects on stomatal conductance, many investigations of water use in trees have shown a decrease in transpiration driven by diminishing stomatal conductance as VPD increases (Monteith 1995; Whitehead 1998). Although we did not measure stomatal conductance, the shape of the J_s response to VPD when normalized by irradiance (see Meinzer *et al*. 1995) showed that J_s initially increased then decreased (Fig. 5). This could indicate that a decline in stomatal conductance with higher evaporative demand occurred only after an initial threshold was reached. The positive correlation occurred only under conditions of very high irradiance or very low VPD, both of which are situations in which stomatal aperture might be expected to be greater. Meinzer *et al*. (1995) and Granier

Table 8. Mean values for the dependent variables tested in the MANCOVA

	Species										
Parameter	*Be*	*Ci*	*Co*	*Dp*	*Ha*	*Hm*	*La*	*Mg*	*Pm*	*Sa*	Overall
n	4	5	4	4	4	4	4	4	8	4	47
y_o	–1.03	–0.62	–0.55	–0.74	–0.88	–0.91	–0.97	–0.58	–0.73	–0.64	–0.76
a	3.49	2.96	2.90	2.55	2.61	3.00	3.28	3.19	2.80	2.99	2.95
x_o	1.08	0.90	0.81	0.34	0.38	0.93	0.78	1.33	0.70	1.16	0.83
b	0.77	0.37	0.28	0.31	0.37	0.55	0.54	0.41	0.40	0.45	0.44
c	0.02	0.01	0.03	0.04	0.01	0.01	0.06	0.00	0.02	–0.03	0.02
R^2	92.3	86.8	87.5	84.7	92.1	90.3	93.1	88.1	89.2	87.9	89.3
Max	0.05	0.40	0.43	–0.07	–0.12	0.20	0.06	0.79	0.17	0.56	0.24
Min	2.11	1.38	1.17	0.73	0.86	1.64	1.48	1.85	1.22	1.74	1.39
Canopy area	110	71	50	200	93	162	202	105	104	97	116
Liana cover	44	0	0	19	3	16	14	63	10	0	15
Height index	0.63	–0.37	–0.17	1.29	–0.22	0.57	0.20	0.12	0.51	1.11	0.37

The species codes are the first letters of the genus and species. The symbols in the parameter column refer to those described in eqn (1). Max and Min refer to the EDI values taken at the points where the second derivative of the equation reached maximum and minimum values. The R^2 values are only a descriptor of model fit and are not used to make any inferences.

Table 9. The results of the analysis of the covariates and the species main effect on the model parameters

Effect	Pillai's trace	*F*	Hypothesis d.f.	Error d.f.	*P*-value
Crown area	0.243	1.005	8	25	0.457
Liana cover	0.438	2.439	8	25	0.042
Canopy height	0.437	2.422	8	25	0.043
Species	2.292	1.428	72	256	0.024

Since the MANCOVA was not significant for crown area, we did not include this variable as a covariate.

et al. (1992) showed the stomatal conductance of three species we studied (*S. amara*, *C. insignis* and *C. obtusifolia*) declined with increasing VPD. Although the majority of our observations would support their results, there did appear to be significant intervals in which VPD did not decrease stomatal aperture if this was the major factor driving transpiration during the initial increase in sap flow seen in Fig. 5. Furthermore, Meinzer *et al*. (1995) showed that in one species, transpiration decreased at high VPD. We never observed this in any of our data, although eddy covariance measurements from La Selva over approximately the same period as our study indicated a slight negative effect of high VPD on ecosystem carbon uptake (Loescher *et al*. 2003). In more seasonal Amazonian forests, VPD has been identified as an important limit on canopy carbon uptake (Grace *et al*. 1995; Mahli *et al*. 1998), but the effect might be more subtle at La Selva due to the extremely wet conditions.

Our results also showed that the study trees at La Selva were probably not limited by soil water because J_s did not

Table 12. The variance explained by the sap flow model (eqn 1) with the parameters estimated from different levels of sample pooling

Species	Mean (standard error) R^2 of models using individual tree data	R^2 of models using data pooled within species	R^2 of model using all data
Be	92.33 (0.78)	90.10	
Ci	86.77 (2.35)	86.16	
Co	87.50 (3.51)	87.74	
Dp	84.71 (3.52)	80.66	
Ha	92.54 (0.67)	89.26	
Hm	90.32 (2.37)	89.63	
La	93.11 (0.41)	85.14	
Mg	88.13 (2.41)	82.28	
Pm	89.20 (1.41)	88.02	
Sa	87.93 (1.16)	85.07	
Mean across species	89.25	86.12	83.82

The first column gives the species name codes. The values in the second column were derived by averaging the R^2 of models on data from individual trees. R^2 values in the third column were derived from data pooled within each species, and the single R^2 value in the fourth column was estimated from the entire set of observations.

Table 10. Univariate ANCOVA results: only dependent variables with significant *F*-tests ($P < 0.05$) are shown

Source	Dependent variable	Sum of squares error	d.f.	Mean square error	*F*	*P*-value
Liana cover	x_o	0.764	1	0.764	8.750	0.006
	Min	0.841	1	0.841	8.389	0.007
	Min	0.632	1	0.632	5.419	0.026
Canopy height	*a*	0.937	1	0.937	7.118	0.012
Species	y_o	0.895	9	0.099	2.924	0.012
	a	2.824	9	0.314	2.385	0.034
	x_o	2.681	9	0.298	3.410	0.005
	b	0.668	9	0.074	6.396	0.000
	Max	2.559	9	0.284	2.836	0.014
	Min	5.231	9	0.581	4.979	0.000

The symbols in the dependent variable column represent the parameters from eqn (1) and the EDI values at the maximum and minimum of the function second derivative.

Table 11. Results of the *post hoc* pair-wise Bonferroni *t*-tests among corrected means

Dependent variable	Results of pair-wise comparisons									
a	Ha^a	Dp^{ab}	Ci^{ab}	Pm^{ab}	Co^{ab}	Hm^{ab}	Mg^{ab}	La^{ab}	Sa^{ab}	Be^b
x_o	Dp^a	Ha^{ab}	La^{ab}	Pm^{ab}	Be^{ab}	Hm^{ab}	Co^{ab}	Mg^{ab}	Ci^{ab}	Sa^b
b	Dp^a	Co^a	Ha^a	Ci^a	Pm^a	Mg^a	Sa^a	La^{ab}	Hm^{ab}	Be^b
Min	Dp^a	Ha^{ab}	Pm^{ab}	Co^{ab}	La^{ab}	Ci^{ab}	Mg^{ab}	Hm^b	Sa^b	Be^b

We only compared the dependent variables with significant mean differences. Species with the same letters in superscript did not differ ($P > 0.05$).

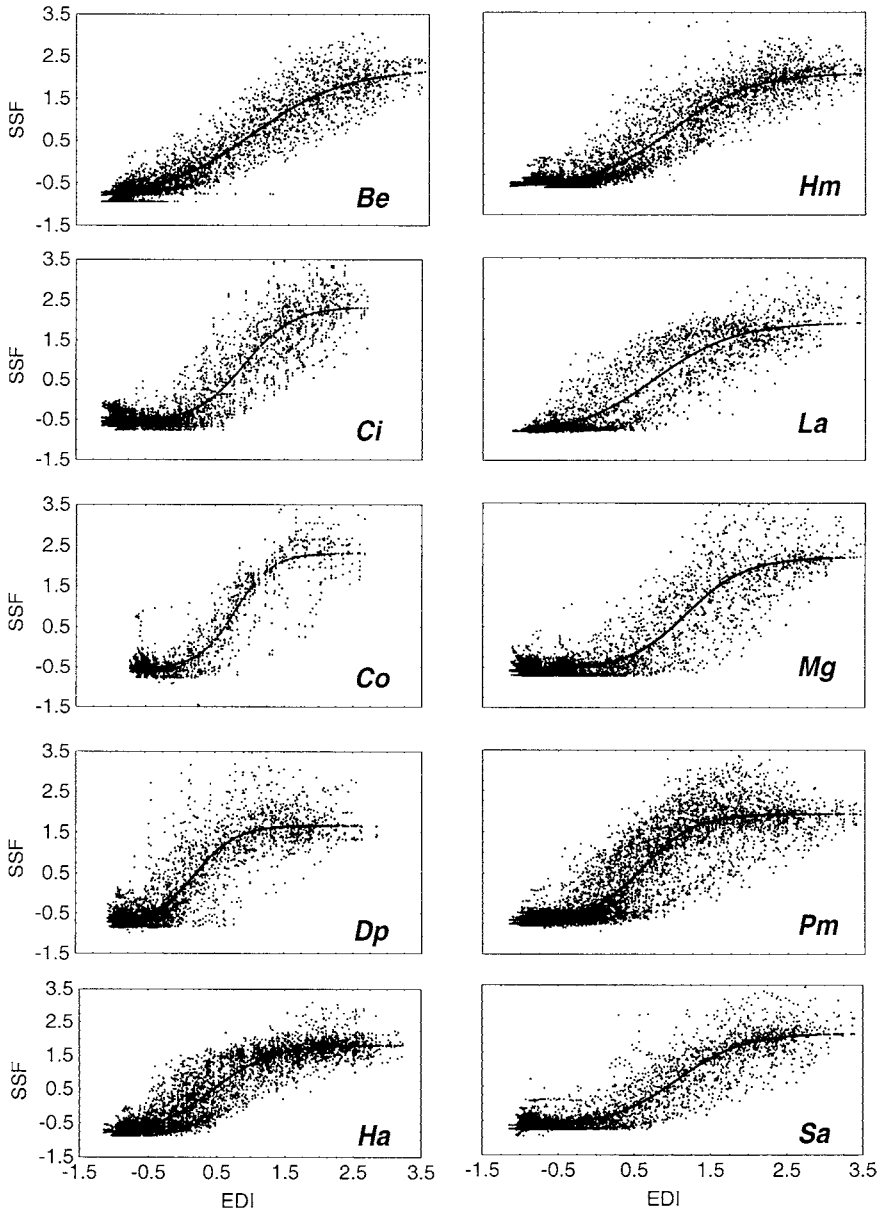

Figure 10. Standardized sap flow (SSF, *Y* axis) plotted against EDI for each of the 10 species. The solid line represents the predicted sap flow of the model calculated from parameters estimated from all individuals pooled within a species. The points are the observed mean 30-min averages of sap flux for all individuals within a species. The letters in the lower right corner of each plot refer to the first letters of the tree genus and species.

respond to changes in soil moisture and never decreased under conditions of high evaporative demand. Granier, Lousteau & Bréda (2000) found a similar response in a study of tree canopy conductance in several different forest types with plentiful soil moisture. However, based on eddy covariance data from Cuieiras, Brazil, Mahli *et al*. (1998) suggested that gross primary productivity in more seasonal forests was probably limited by soil moisture. Using sensitivity analysis, Williams *et al*. (1998) identified soil moisture and soil/root hydraulic resistance as two of the primary climatic controls on evapotranspiration for the same site in Brazil.

Liana cover varied among the study trees and across species. Liana presence in a tree crown and the tree's crown position relative to the canopy neighbourhood had a significant effect on sap flow responses. Heavy liana cover in the crown delayed the tree sap flow response to conditions of higher evaporative demand, probably through shading by liana leaves. This shading might also explain the negative impact on growth by lianas shown by Clark & Clark (1990) in several of the taxa we report on here. Trees with emergent crowns reached maximum sap flow under conditions of lower evaporative demand than trees embedded in the canopy. Even though we intended to minimize the variance in crown characteristics through our sampling strategy, tree canopy idiosyncrasies were still an important source of variation in the model parameter estimates. These characteristics would probably become more important as these trees matured, since several species (all the emergent species) we measured had not achieved their full stature.

Many authors have reported lags between sap flow measured at the base of trees and transpiration in the crown (e.g. Landsberg, Blanchard & Warrit 1976; Granier & Lousteau 1994; Goldstein *et al*. 1998; Phillips *et al*. 1999; but see

Ewers & Oren 2000). The morning lag in J_s in response to light that we observed might be explained by water capacitance in the stem, a slow stomatal response to light, boundary layer dynamics, or diffusion limited by wet leaves. Leaf wetness appeared to be important in explaining the morning lag in J_s response to irradiance. The diurnal pattern of leaf wetness shows rapid drying of wet leaves occurring over the same period that we observed the lag in J_s response to light. The afternoon lag in VPD response seen as hysteresis in Fig. 4b could be driven by stomatal closure either in response to higher VPD, decreasing light levels, or internal cycles. An example of the latter is the clockwork closure of leaflets (and stomata) of *P. macroloba* in the afternoon whereas irradiances are still relatively high (Oberbauer, Strain & Riechers 1987). Interestingly, the combination of morning lags in response to light and afternoon lags in response to VPD resulted in much smaller overall hysteresis when *SSF* was plotted against EDI (Fig. 4c).

Climate change scenarios suggest that rainfall and soil moisture levels will decline and seasonality will increase in many areas of the Neotropics, although in some areas, such as Central America, rainfall is predicted to increase (Hulme & Viner 1998). If changing climate dried the soil to the point where water became limited, the upper asymptote in sap flow rates shown by our model might disappear. Soil water limitations would then cause a decrease in transpiration under conditions of high evaporative demand. If conditions became wetter, wet leaves and lower light levels might lower sap flow rates. Morphological and architectural differences among the species might interact differently under these conditions. While we cannot examine these scenarios easily, the common sap flow response at the scale we measured (whole tree) did not vary greatly under current conditions. External factors such as liana cover and crown position had more impact on tree water use than species-specific characteristics. Our model of sap flux response to the evaporative demand index proved more effective than individual environmental variables for predicting short-term tree water use across species, but when integrating measurements over an entire day, VPD explains nearly as much variation as the composite index. This is probably because lags and hysteresis among the environmental variables become less important when averaged over a day. Nevertheless, our approach offers a simple way to examine how weather influences short-term tree water use responses, to compare these responses among species, and to project sap flux rates through time. The similarity among sap flux responses of the study trees suggests that variation in climate will affect whole-tree photosynthesis of the study species similarly, a finding compatible with the synchronous growth responses of many of these species to climate variation (Clark & Clark 1994; Clark *et al*. 2003). Clark & Clark (1994) showed species growth responses appeared similar but the magnitude of the growth rates varied among the species. Understanding the variability in water use efficiency and carbon allocation among these species would explain their different growth rates and help predict how these forests might respond to climate change.

ACKNOWLEDGMENTS

This paper represents contribution number 72 to the programme in tropical biology at Florida International University. This work was funded jointly by the National Science Foundation (DEB-9629245), the US Department of Energy (IBN-9652699), and Florida International University Tropical Biology Program. We thank Henry Loescher for providing part of the weather data. We thank Jason Drake and Matthew Clark for the LIDAR and GIS data. Sylvia Englund and Maureen Donnelly, and two anonymous reviewers provided valuable editorial comments. We would like to thank the Organization for Tropical Studies for logistical support.

REFERENCES

Andrade J.L., Meinzer F.C., Goldstein G., Holbrook N.M., Cavelier J., Jackson P. & Silvera K. (1998) Regulation of water flux through trunks, branches, and leaves in trees of a lowland tropical forest. *Oecologia* **115,** 463–461.

Campbell G.S. & Norman J.M. (1998) *An Introduction to Environmental Biophysics*. Springer-Verlag, New York, USA.

Clark D.A. & Clark D.B. (1992) Life history diversity of canopy and emergent trees in a neotropical rain forest. *Ecological Monographs* **62,** 315–344.

Clark D.A. & Clark D.B. (1994) Climate-induced annual variation in canopy tree growth in a Costa Rican tropical rain forest. *Journal of Ecology* **82,** 865–872.

Clark D.A. & Clark D.B. (1999) Assessing the growth of tropical rain forest trees: issues for forest modeling and management. *Ecological Applications* **9,** 981–997.

Clark D.A., Piper S.C., Keeling C.D. & Clark D.B. (2003) Tropical rain forest tree growth and atmospheric carbon dynamics linked to interannual temperature variation during 1984–2000. *Proceedings of the National Academy of Sciences of the USA* **100,** 5852–5857.

Clark D.B. & Clark D.A. (1990) Distribution and effects on tree growth of lianas and hemiepiphytes in a Costa Rican tropical wet forest. *Journal of Tropical Ecology* **6,** 321–331.

Clearwater M.J., Meinzer F.C., Andrade J.L., Goldstein G. & Holbrook N.M. (1999) Potential errors in measurement of nonuniform sap flow using heat dissipation probes. *Tree Physiology* **19,** 681–687.

Drake J.B., Dubayah R.O., Clark D.B., Knox R.G., Blair J.B., Hofton M.A., Chazdon R.L., Weishampel J.F. & Prince S.D. (2002) Estimation of tropical forest structural characteristics using large-footprint lidar. *Remote Sensing of Environment* **79,** 305–319.

Ewers B.E. & Oren R. (2000) Analysis of assumptions and errors in the calculation of stomatal conductance from sap flow measurements. *Tree Physiology* **20,** 579–589.

Fetcher N., Oberbauer S.F. & Chazdon R.L. (1994) Physiological ecology of trees, shrubs, and herbs at La Selva. In: *La Selva: Ecology and Natural History of a Neotropical Rainforest* (eds L.A. McDade, K.S. Bawa, H.A. Hespenheide & G.S. Hartshorn), pp. 128–141. University of Chicago Press, Chicago, IL, USA.

Frankie G.W., Baker H.G. & Opler P.A. (1974) Comparative phenological studies of trees in tropical wet and dry forests in the lowlands of Costa Rica. *Journal of Ecology* **62,** 881–919.

Goldstein G., Andrade J.L., Meinzer F.C., Holbrook N.M., Cavelier J., Jackson P. & Celis A. (1998) Stem water storage and

diurnal patterns of water use in tropical forest canopy trees. *Plant, Cell and Environment* **21,** 397–406.

Grace J., Lloyd J., McIntyre J., Miranda A.C., Meir P., Miranda H.S., Moncrieff J., Massheder J., Wright I. & Gash J. (1995) Fluxes of carbon dioxide and water vapor over an undisturbed tropical forest in south-west Amazonia. *Global Change Biology* **1,** 1–12.

Granier A. (1987) Evaluation of transpiration in a Douglas fir stand by means of sap flow measurements. *Tree Physiology* **3,** 309–320.

Granier A. & Lousteau D. (1994) Measuring and modelling the transpiration of a maritime pine canopy from sap-flow data. *Agricultural and Forest Meteorology* **71,** 61–81.

Granier A., Huc R. & Colin F. (1992) Transpiration and stomatal conductance of two rain forest species growing in plantations (*Simarouba amara* and *Goupia glabra*) in French Guyana. *Annals of Forest Science* **49,** 17–24.

Granier A., Lousteau D. & Bréda N. (2000) A generic model of forest canopy conductance dependent on climate, soil water availability and leaf area index. *Annals of Forest Science* **57,** 755–765.

Gutierrez M.V., Harrington R.A., Meinzer F.C.A. & Fownes J.H. (1994) The effect of environmentally induced stem temperature gradients on transpiration estimates from the heat balance method in two tropical woody species. *Tree Physiology* **14,** 179–190.

Hulme M. & Viner D. (1998) A climate change scenario for the tropics. *Climatic Change* **39,** 145–176.

Jarvis P.G. & McNaughton K.G. (1986) Stomatal control of transpiration: scaling up from leaf to region. *Advances in Ecological Research* **15,** 1–49.

Jiménez M.S., Nadezhdina N., Čermák J. & Morales D. (2000) Radial variation in sap flow in five laurel forest tree species in Tenerife, Canary Islands. *Tree Physiology* **20,** 1149–1156.

King D.A. (1996) Allometry and life history of tropical trees. *Journal of Tropical Ecology* **12,** 25–44.

Landsberg J.J., Blanchard T.W. & Warrit B. (1976) Studies on the movement of water through apple trees. *Journal of Experimental Botany* **27,** 579–596.

Loescher H.W., Oberbauer S.F., Gholz H.L. & Clark D.B. (2003) Environmental controls on net ecosystem-level carbon exchange and productivity in a Central American tropical wet forest. *Global Change Biology* **9,** 396–412.

Mahli Y., Nobre A.D., Grace J., Kruijt B., Pereira M.G.P., Culf A. & Scott S. (1998) Carbon dioxide transfer over a Central Amazonian rain forest. *Journal of Geophysical Research* **103,** 31,593–31,531,612.

Meinzer F.C. & Andrade J.L. (1997) Control of transpiration from the upper canopy of a tropical forest: the role of stomatal, boundary layer and hydraulic architecture components. *Plant, Cell and Environment* **20,** 1242–1252.

Meinzer F.C., Goldstein G. & Andrade J.L. (2001) Regulation of water flux through tropical forest canopy trees: do universal rules apply? *Tree Physiology* **21,** 19–26.

Meinzer F.C.A., Goldstein G., Holbrook N.M., Jackson P. & Cavelier J. (1993) Stomatal and environmental control of transpiration in a lowland tropical forest tree. *Plant, Cell and Environment* **16,** 429–436.

Meinzer F.C., Goldstein G., Jackson P., Holbrook N.M., Gutiérrez M.V. & Cavelier J. (1995) Environmental and physiological regulation of transpiration in tropical forest gap species: the influence of boundary layer and hydraulic properties. *Oecologia* **101,** 514–522.

Monteith J.L. (1995) A reinterpretation of stomatal responses to humidity. *Plant, Cell and Environment* **18,** 357–364.

Oberbauer S.F., Strain B.R. & Riechers G.H. (1987) Field water relations of a wet-tropical forest tree species, *Pentaclethra macroloba* (Mimosaceae). *Oecologia* **71,** 369–374.

Phillips N., Oren R., Zimmermann R. & Wright S.J. (1999) Temporal patterns of water flux in trees and lianas in a Panamanian moist forest. *Trees: Structure and Function* **14,** 116–123.

Ryan M.G., Hubbard R.M., Clark D.L. & Sanford R.L. Jr (1994) Woody tissue respiration for *Simarouba amara* and *Minquartia guianensis*, two tropical wet forest trees with different growth habits. *Oecologia* **100,** 213–220.

Smith W.K. & McClean T.M. (1989) Adaptive relationship between leaf water repellency, stomatal distribution, and gas exchange. *American Journal of Botany* **76,** 465–469.

Walter H. (1985) *Vegetation of the Earth and Ecological Systems of the Geo-Biosphere*, 3rd edn. Springer-Verlag, Berlin, Germany.

Weishampel J.F., Blair J.B., Knox R.G., Dubayah R. & Clark D.B. (2000) Volume tric lidar return patterns from an old-growth tropical rainforest canopy. *International Journal of Remote Sensing* **21,** 409–415.

Whitehead D. (1998) Regulation of stomatal conductance and transpiration in forest canopies. *Tree Physiology* **18,** 633–644.

Williams M., Bond B. & Ryan M.G. (2001) Evaluating different soil and plant hydraulic constraints on tree function using a model and sap flow data from ponderosa pine. *Plant, Cell and Environment* **24,** 679–690.

Williams M., Mahli Y., Nobre A., Rastetter E.B., Grace J. & Pereira M.G.P. (1998) Seasonal variation in net carbon exchange and evapotranspiration in a Brazilian rain forest: a modeling analysis. *Plant, Cell and Environment* **21,** 953–968.

Received 23 July 2003; received in revised form 13 November 2003; accepted for publication 17 November 2003